

CONF-970135-3

SAND--96-2603C

RECEIVED

NOV 20 1996

OSTI

# Damage Estimates from Long-Term Structural Analysis of a Wind Turbine in a U.S. Wind Farm Environment

MASTER

Neil D. Kelley  
Herbert J. Sutherland

*Prepared for  
1997 ASME Wind Energy Symposium  
Reno, Nevada  
January 6-9, 1997*



National Renewable Energy Laboratory  
1617 Cole Boulevard  
Golden, Colorado 80401-3393  
A national laboratory of the U.S. Department of Energy  
Managed by Midwest Research Institute  
for the U.S. Department of Energy  
under contract No. DE-AC36-83CH10093

Prepared under Task No. WE618010

October 1996

DISTRIBUTION OF THIS DOCUMENT IS UNLIMITED

ML

## **NOTICE**

This report was prepared as an account of work sponsored by an agency of the United States government. Neither the United States government nor any agency thereof, nor any of their employees, makes any warranty, express or implied, or assumes any legal liability or responsibility for the accuracy, completeness, or usefulness of any information, apparatus, product, or process disclosed, or represents that its use would not infringe privately owned rights. Reference herein to any specific commercial product, process, or service by trade name, trademark, manufacturer, or otherwise does not necessarily constitute or imply its endorsement, recommendation, or favoring by the United States government or any agency thereof. The views and opinions of authors expressed herein do not necessarily state or reflect those of the United States government or any agency thereof.

Available to DOE and DOE contractors from:

Office of Scientific and Technical Information (OSTI)  
P.O. Box 62  
Oak Ridge, TN 37831

Prices available by calling (423) 576-8401

Available to the public from:

National Technical Information Service (NTIS)  
U.S. Department of Commerce  
5285 Port Royal Road  
Springfield, VA 22161  
(703) 487-4650



Printed on paper containing at least 50% wastepaper, including 20% postconsumer waste

#### **DISCLAIMER**

**Portions of this document may be illegible  
in electronic image products. Images are  
produced from the best available original  
document.**

# DAMAGE ESTIMATES FROM LONG-TERM STRUCTURAL ANALYSIS OF A WIND TURBINE IN A U.S. WIND FARM ENVIRONMENT\*†

Neil D. Kelley  
National Wind Technology Center  
National Renewable Energy Laboratory  
Golden, Colorado 80401

Herbert J. Sutherland  
Wind Energy Department  
Sandia National Laboratory  
Albuquerque, NM 87185

## ABSTRACT

Time-domain simulations of the loads on wind energy conversion systems have been hampered in the past by the relatively long computational times for nonlinear structural analysis codes. However, recent advances in both the level of sophistication and computational efficiency of available computer hardware and the codes themselves now permit long-term simulations to be conducted in reasonable times. Thus, these codes provide a unique capability to evaluate the spectral content of the fatigue loads on a turbine. To demonstrate these capabilities, a Micon 65/13 turbine is analyzed using the YawDyn and the ADAMS dynamic analysis codes. The SNLWIND-3D simulator and measured boundary conditions are used to simulate the inflow environment that can be expected during a single, 24-hour period by a turbine residing in Row 41 of a wind farm located in San Gorgonio Pass, California. Also, long-term simulations (up to 8 hours of simulated time) with constant average inflow velocities are used to better define the characteristics of the fatigue load on the turbine. Damage calculations, using the LIFE2 fatigue analysis code and the MSU/DOE fatigue data base for composite materials, are then used to determine minimum simulation times for consistent estimates of service lifetimes.

## INTRODUCTION

Considerable progress has been made in the simulation of the dynamic response of operating wind turbines over the past several years. Part of the progress can be attributed to the ability to simulate more realistically the three-dimensional structure of the turbulent inflow. Further, with recent advances in the level of sophistication of the codes themselves and the availability of faster and more efficient computers, the computationally-demanding, highly nonlinear processes related to structural loads now can be performed in reasonable times. When excited by a realistic turbulent inflow, the currently available dynamics codes are capable of predicting the distribution of fatigue loads on a wind turbine; e.g., see the recent study by Kelley, et al.<sup>1</sup> in which predicted and observed blade flapwise load distributions are compared for rigid and teetered hub designs using long-term inflow simulations. In this paper we expand on that study by utilizing long-term simulations of a Micon 65/13 turbine located in a U.S. wind park. The turbine is simulated using the SNLWIND-3D, YawDyn, and ADAMS<sup>‡</sup> numerical codes to predict fatigue damage. The damage is determined using the LIFE2 fatigue analysis code and the MSU/DOE fatigue data base for composite materials.

Three long term simulations of the Micon 65/13 turbine are used in the damage calculations presented here. The first is a 24-hour simulation of the turbine in Row 41 of a U.S. wind park. This simulation, which used the ADAMS code, is based on the measured diurnal inflow at this location. The second is an 8-hour

\*This work is supported by the U.S. Department of Energy under Contract DE-AC04-94AL85000 and DE-AC36-83CH10093.

†This paper is declared a work of the U.S. Government and is not subject to copyright protection in the United States.

‡ ADAMS is a registered trademark of Mechanical Dynamics, Inc.

simulation of the turbine using the YawDyn code at Row 41 of the wind park with an approximately constant average inflow velocity of 12.5 m/s. The third and final simulation is an 8-hour simulation using the YawDyn code at Row 37 of the wind park with the same approximately constant average inflow velocity of 12.5 m/s. This final calculation permits a direct comparison of the simulation to measured turbine load data. The two 8-hour simulations yield significantly different results because Row 37 is one row, i.e., 7 rotor diameters (7D), down-wind of working turbines and Row 41 is 14D downwind. Thus, the wake effects on the Row 37 turbine will be greater than the wake effects on the Row 41 turbine.

### **ANALYSIS CODES USED IN THIS STUDY**

A total of four numerical codes were used in this experiment. These included the SNLWIND-3D turbulent inflow simulation,<sup>2</sup> the YawDyn/AeroDyn<sup>3</sup> and ADAMS<sup>4</sup> structural dynamics codes, and the LIFE2 Fatigue Analysis code.<sup>5</sup>

### **Structural Models of the Turbine**

The turbine studied here is a Micon 65/13 three-bladed, rigid-hub turbine installed in Row 37 of a 41-row wind farm in San Gorgonio Pass, California. This stall-controlled turbine has an upwind rotor with a diameter of 17 m and was fitted with blades using airfoil shapes from the NREL (SERI) thin-airfoil family.<sup>6</sup> The turbine has active yaw.

For the purpose of this study, the Micon turbine was simulated with fixed yaw; thus, the YawDyn analysis had three degrees-of freedom (DOF); i.e., first flapwise mode for each of the three blades. This model of this turbine was developed by Laino<sup>7</sup> and was based, in part, on the earlier ADAMS model developed by Buhl et al.<sup>8</sup> The ADAMS model, as applied in this study, took advantage of the refined blade aerodynamic properties incorporated by Laino<sup>7</sup> in his modeling of the turbine. As implemented in this study, the ADAMS model contained 310 DOF. The AeroDyn subroutines used for both the YawDyn and ADAMS simulations included the options of dynamic stall and inflow. The structural codes have been reasonably well validated by Laino and Kelley<sup>7</sup> and Kelley et al.<sup>1</sup>

### **Simulated Inflows**

**Diurnal simulation:** In this paper we have taken advantage of the long-term, 24-hour simulation conducted by Kelley et al.<sup>1</sup> This diurnal record consisted of 144 10-minute records of representative

turbulent inflow conditions that are likely to be seen in the last downwind row of a large 41-row wind farm in San Gorgonio Pass, California. The SNLWIND-3D turbulence spectral model used to develop the simulations for this study is based on extensive boundary layer measurements collected at Row 41 during the 1989 wind season. At that time more than 900 wind turbines were installed ahead of this row. The closest operating turbines to this location were two rows or 14 rotor diameters (14D) upstream. The model was supplemented by measurements taken upstream of two working Micon 65 turbines in Row 37 (7D upstream rotor spacing) during the 1990 season. The components of the three-dimensional wind vector were simulated at a rate of 20 per second on a 6x6 Cartesian grid and at the rotor center, scaled to the rotor diameter of the Micon 65. See Kelley et al.<sup>1</sup> for a discussion of the process used to generate the diurnal simulation. The frequency distribution of the diurnal variation of simulated, 10-minute hub-height mean wind speeds is shown in Figure 1.

**8-hour Simulations:** Two 8-hour simulations were required, one at Row 41 and one at Row 37. Row 41 was chosen for the diurnal simulation because of the extensive meteorological record available at this row. Unfortunately, no accompanying turbine loads data were available. However, measured loads data were available upstream at Row 37. The significant difference between Row 37 and Row 41 is that turbines were operating 7D upstream of Row 37 and 14D upstream of Row 41. Thus, the simulation at Row 37 can be compared directly to measured data, and the simulation at Row 41 can be used to investigate the diurnal variation of the fatigue loads on a turbine.

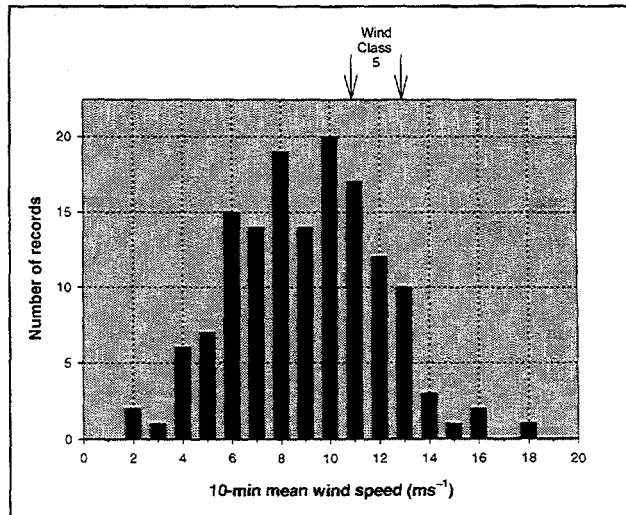


**Figure 1. Simulated diurnal 10-minute mean wind speed distributions.**

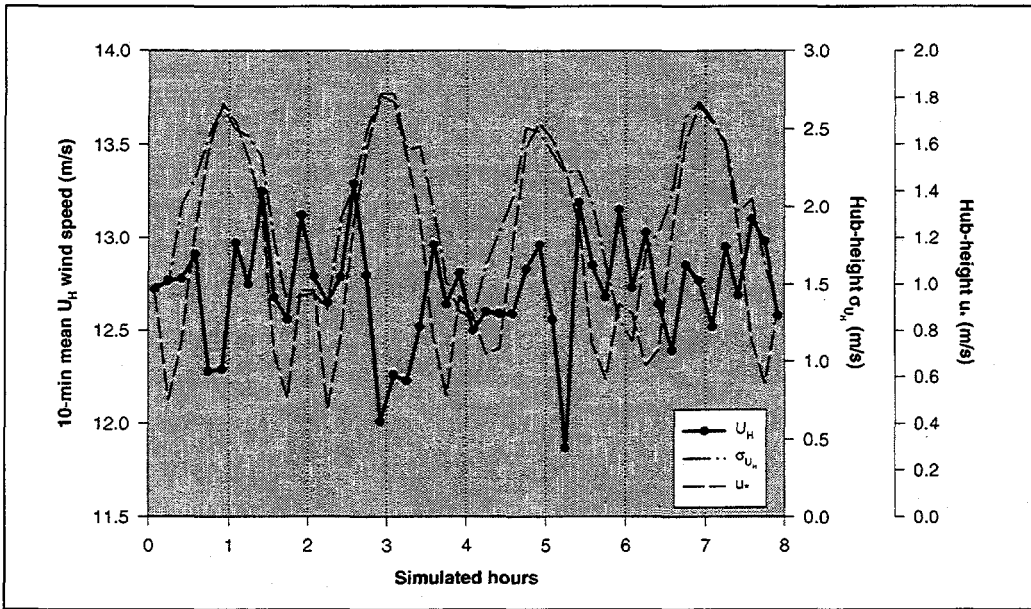


Figure 2. Variation of the turbulence parameters in the 8-hour Row 41 simulation.

We have found, from our experience in analyzing extensive wind records from a number of active wind sites installed in widely varying terrain, that the statistics for the inflow to a wind turbine can be considered quasi-stationary only over a period of approximately 8-12 minutes. For record lengths of less than 8 minutes, the data sample is not sufficient to produce statistical convergence. For periods longer than about 12 minutes, larger-scale atmospheric phenomena and diurnal changes in the turbulence scaling parameters associated with atmospheric boundary layer combine to again increase the statistical variability. The turbulence statistics within a wind farm flow never reach convergence because of the evolutionary nature of the decaying upstream turbine wakes and their interaction with the freestream, see Højstrup and Nørgård.<sup>9</sup> As a result, it is not possible to obtain a long time series of several hours of experimental data that can be considered quasi-steady. However, long records with constant turbulent scaling parameters can be obtained through simulations. These long records are useful for assessing the impact on fatigue damage of the various approaches to cycle-counting load histories. They are also very useful for comparing calculated load histories when it is desired that the changes in wind speed during the run be minimal. For our purposes, an 8-hour simulation at Rows 37 and 41 was required.

We could not calculate the 8-hour simulations directly because of computer memory limitations.

However, by concatenating two 4-hour records, we were able to obtain quasi-steady, continuous inflow records of 8-hour duration. Other techniques to join these two simulations could have been used, e.g., tapering the ends of the two records to form a relatively smooth transition. However, the boundary discontinuity created by the concatenation was less than the peak sample-to-sample variations seen within the individual records themselves.

Figure 2 plots the variation of the 10-minute means of the simulated hub-height horizontal wind speed ( $U_H$ ) and the turbulence parameters of standard deviation ( $\sigma_{U_H}$ ) and local mean shearing stress or friction velocity ( $u_*$ ) over the concatenated 8-hour period for a 12.5 m/s mean wind speed at Row 41. As illustrated in this figure, some relatively long term cycles (the order of two hours) are observed in the data. It is not clear why this cyclic behavior appears in these parameters.

An examination of the time series plotted in Figure 2 and a summation of the statistics of the critical turbulence parameters in Table 1 demonstrate that the turbulence characteristics of each of the 4-hour records are similar but not identical. The friction velocity,  $u_*$ , represents the local mean shearing stress measured at hub-height and is defined by:

$$u_* = \left( -u'w' \right)^{1/2}, \quad [1]$$

where  $u'$  and  $w'$  represent the zero-mean longitudinal and vertical velocity components of the wind vector.<sup>2</sup>

Table 1. Turbulence statistics associated with each of the Row 41 4-hour simulations.

Turbulent Parameter	1 <sup>st</sup> 4-hour period	2 <sup>nd</sup> 4-hour period
Mean horizontal wind speed (m/s)	12.71	12.71
Horizontal wind speed standard deviation (m/s)	2.099	2.051
Friction velocity, $u_*$ (m/s)	1.049	1.017
Friction velocity standard deviation (m/s)	1.890	1.854

### Fatigue Damage

The LIFE2 code<sup>5</sup> is a fatigue/fracture mechanics code that is specialized to the analysis of wind turbine components. It is a PC-based, menu-driven code that leads the user through the input definitions required to predict the service lifetime of a turbine component. In the current formulation, the service lifetime of turbine components may be predicted using either Miner's rule or a linear-elastic crack propagation rule. Only Miner's rule is used here.

The LIFE2 code requires four sets of input variables: 1) the wind speed distribution for the turbine site as an average annual distribution, 2) the material fatigue properties required by the damage rule being used to predict the service lifetime of the component, 3) a joint distribution of mean stress and stress amplitude (stress states) for the various operational states of the turbine, and 4) the operational parameters for the turbine and the stress concentration factor(s) for the turbine component. The third set of input variables are "cycle count matrices" that define the operational states of the turbine. We used the long time series discussed above to calculate the fatigue loads on the turbine.

Wind Speed Distribution: For the discussion presented here, this aspect of the program is disabled. Rather than using a typical annual wind speed distribution to predict the service lifetime, we will only examine the damage rate predicted by the 24- and 8-hour simulations. The damage is simply the fraction of the service lifetime consumed by a particular load history.

Material Fatigue Properties: The fatigue life analysis used here is based on Miner's rule. In this linear damage rule, the accumulated damage from each stress cycle requires that the number of cycles to failure be described as a function of cycle mean and amplitude. For many materials this function, typically called an S-n diagram, may be posed mathematically using Goodman or Gerber models or graphically using a Goodman diagram. For this analysis, we will use the Goodman diagram determined by Sutherland and Mandell<sup>10</sup> from the S-n data developed by

Mandell et al.<sup>11</sup> This characterization of the fatigue behavior of fiberglass composite materials that are typically used in wind turbine blades is shown in Figure 3.

Another typical representation of these data is to fit them with a power law of the form:

$$\varepsilon = C N^{-\frac{1}{m}}, \quad [2]$$

where  $\varepsilon$  is a measure of the cyclic strain,  $N$  is the number of cycles to failure, and  $m$  and  $C$  are the curve fitting parameters. As illustrated by Sutherland and Mandell,<sup>10</sup> the fatigue exponent  $m$  for these fits is always greater than 10. Thus, these materials are said to have a high fatigue exponent. Materials, such as metals, with fatigue exponents of 2 or 3 are said to have a low fatigue exponent.

Normal Operation Loads: As discussed above, four sets of the normal operation loads are available for this analysis: the three load spectra obtained by rainflow counting the simulations described above and the rainflow counted, measured load spectrum from the Micon 65 turbine located in Row 37 of the wind park.

For the LIFE2 fatigue analyses presented here, the normal operation loads on the turbine were described by a series of operational stress states (cycle-count

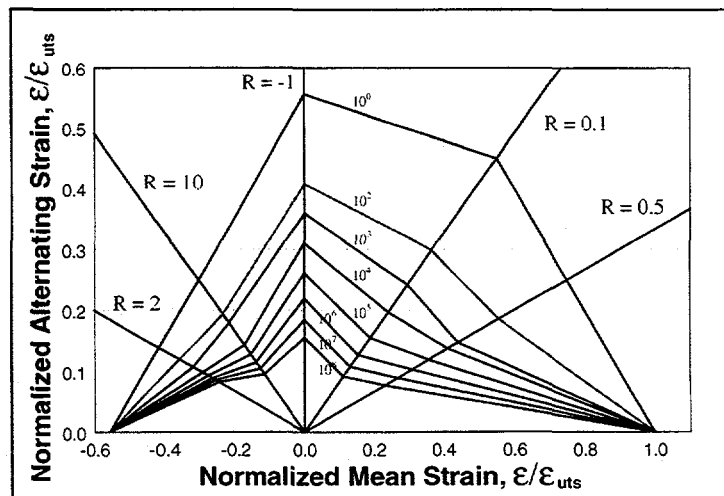


Figure 3. Normalized Goodman diagram for fiberglass composites.

matrices) that were based on the wind speed class of the inflow. These operational states were constructed by categorizing each 10-minute record contained in an operational load set by its hub-height mean wind speed,  $U_H$ . Wind Class 3 includes speeds less than 9 m/s whereas Classes 4, 5, 6, and 7 encompass ranges of 9-11, 11-13, 13-15, and 15-17 m/s, respectively. Records with a mean speed greater than 17 m/s are assigned to Class 8. Loads from starting and stopping the turbine and buffeting by high winds are not considered in this investigation.

**Rainflow Counting:** The time-histories of the operational blade loads were converted to fatigue cycles using a version of the Downing and Socie<sup>12</sup> rainflow counting algorithm. The algorithm produces cycle count matrices that are a joint distribution of mean stress and stress amplitude (stress states) for the various operational states of the turbine. In this version of the algorithm,<sup>13</sup> all half-cycles are closed and counted as full cycles.

**Damage Calculations:** To convert the blade fatigue loads (cycle-count matrices) to material strains, we have used the technique previously used by Sutherland and Kelley<sup>14</sup> to analyze these turbines. We assumed that these blades are based on a maximum strain design of 0.4 percent (commonly used in the wind industry by blade designers); namely, that the nominal strain levels are not allowed to exceed this value. We assumed that this value occurs at the average value of the Wind Class 7 load spectrum plus 4 standard deviations. Further, we assume that the nominal strain is subjected to a stress concentration factor of 2.5. The result of these assumptions is to place the maximum load cycle observed in all the spectra at approximately the 500 cycles-to-failure level and the body of the distributions in the  $10^7$  to  $10^8$  cycles-to-failure range. As these assumptions have significant implications on the predicted fatigue lifetime and they were not used in the actual design of these blades, we will only report results of our parametric study in nominal damage, i.e., the ratio of the damage to an average value of the damage (damage is the reciprocal of the service lifetime). This ratio provides the comparison we need while minimizing the effects of these assumptions.

#### **COMPARISONS WITH EXPERIMENTAL DATA**

As discussed above, measured load histories are available for a Micon turbine located in Row 37 of the wind farm. We identified a subset of 14 10-minute records in which the observed hub mean wind speed was  $12.5 \pm 0.1$  m/s. We chose this

mean wind speed because it corresponds to the peak power for the NREL thin-airfoils blades. At this wind speed, one can expect considerable unsteady aerodynamic and aeroelastic response as the outer portions of the blades cycle in and out of stall. This value is also within a range of speeds specified as Wind Class 5 ( $11 \leq U_H < 13$  m/s, where  $U_H$  is the average horizontal hub-height wind speed) where Sutherland and Kelley<sup>14</sup> found the greatest fatigue damage accumulation at Row 37.

These data permit a direct comparison of the simulations to measured data.

#### **Structural Loads**

The measured loads data were compared to the two 4-hour simulations at Row 37 that were obtained by using SNLWIND-3D simulation to generate the inflow and the Micon 65 YawDyn model to predict flapwise loads. Figure 4 summarizes the predicted and observed alternating flapwise load spectra. As illustrated in this figure, the measured and the predicted spectra differ in the very important low-cycle, high-amplitude (LCHA) tail (the right-hand side of the figure) where a decaying exponential:

$$N = \alpha_0 e^{-\alpha_1}, \quad [3]$$

is shown fitted to the distribution.

Figure 4 also illustrates that the SNLWIND-

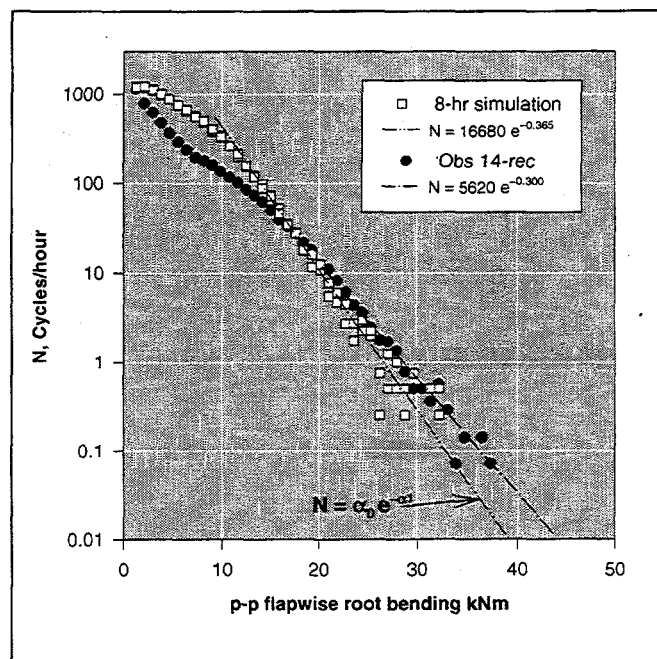


**Figure 4. Comparison of the measured and simulated load distributions at Row 37.**

3D/YawDyn simulation overpredicts the number of cycles in the main body of the distribution (the left-hand side of the figure). The additional cycles in this region are probably a consequence of differences between the turbine and its YawDyn model. The turbine has active yaw while the model assumed that the yaw axis is held fixed. Tangler et al.<sup>15</sup> found, with the yaw drive locked, that the flapwise moment increased due to cyclic loads associated with a strong 4-per-revolution (4P) load superimposed on the once-per-revolution (1P) cyclic load. This 4P contribution to the cyclic load essentially disappears and the flapwise loads decrease when the yaw drive is active. We believe it is this 4P contribution that accounts for the differences in the measured and simulated spectra in the main body of the distribution shown in Figure 4.

### Damage

The damage associated with the measured load histories and the 8-hour simulation were determined using the techniques described above. The results of these calculations are plotted as the damage rate per record (i.e., the damage per 10 minutes) in Figure 5. In this plot, the damage rate is normalized to the average damage rate obtained from the 48 10-minute simulations using the YawDyn simulation, i.e., the 8-hour simulation described above. The average nominal damage rate versus number of 10-minute records included in the average is used to illustrate the trajectory of the accumulated damage to the average nominal damage. As discussed later, this trajectory is important to the determination of the minimum simulation time.

As illustrated here, the damage rate based on measured data is approximately 7.5 times larger than the damage determined from the simulated data. Thus, the simulation significantly underestimates the measured damage rate. At this point, the cause(s) of this discrepancy is not known. However, we note that there are known differences between the structural model and the turbine and that the inflow does not include the time-varying influence of stability and vertical mean shear. This non-inclusive list could easily produce the discrepancy in the damage predictions noted here.

### COMPARISON OF LOAD SPECTRA

The relatively long time series resulting from the structural analyses described above offer a unique chance to examine the details of the load spectrum imposed upon a wind turbine blade. In this section, we will use these time series to address two questions that have been raised by the fatigue analysis community, see Sutherland and Butterfield.<sup>16</sup> The first discussion addresses the question of how long the time series must be to obtain a representative sample of the load spectra imposed upon the blade. And, second, we address the question of how "long" time series may be constructed from many "short" time series. Damage calculations (i.e., prediction of fatigue lifetimes) are used to evaluate answers to these two questions.

For this section of the paper we will only examine the Wind Class 5 wind speed data (i.e., those data and simulations with average inflow wind speeds between 11 and 13 m/s). The 24-hour simulation at Row 41 contained 37 10-minute records, the 8-hour simulations at Rows 37 and 41 contained 48, and the experimental data set taken at Row 37 contained 14.

### Representative Sample

The basic premise in the fatigue calculations is that the cycle count matrix used to describe a particular operational state of the turbine constitutes a representative sample of the fatigue cycles for that operational state. As shown in Figure 6a, the

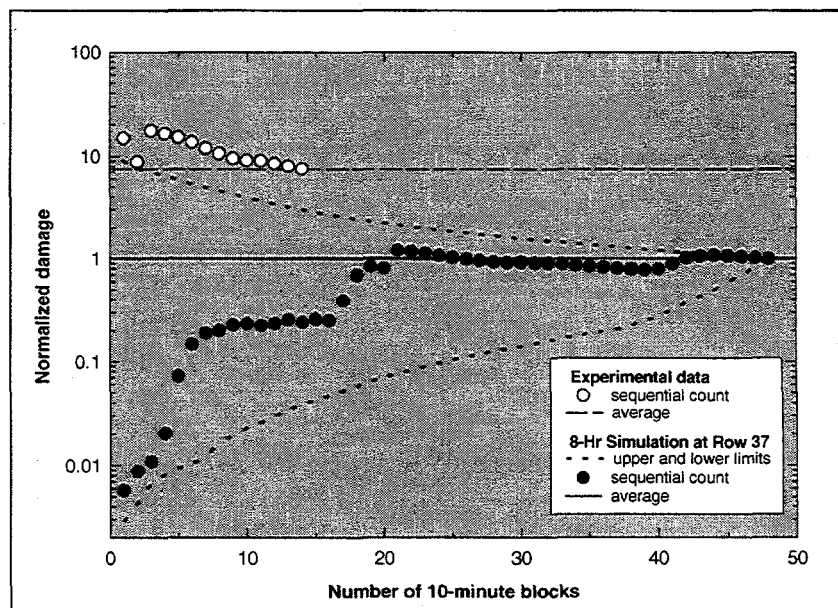
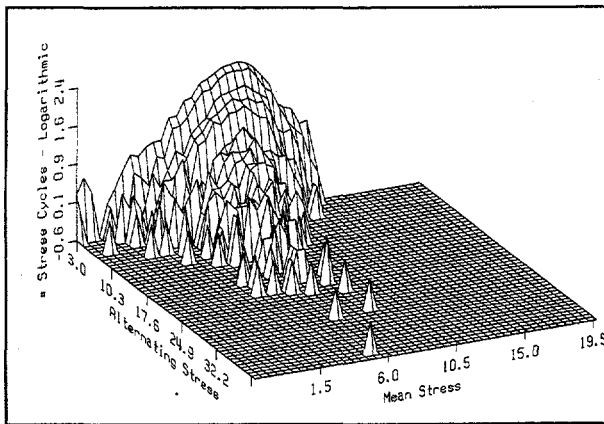


Figure 5. Row 37 normalized damage trajectory using experimental data and the 8-hour simulation.



**Figure 6a. Cycle count matrix based on one 10-minute simulation.**

distribution of fatigue cycles at Row 41 for a 10-minute simulation of a Class 5 wind speed inflow is not very smooth and the high stress tail of the distribution (the LCHA load range) is not filled. Because one expects the distribution to be a smooth, monotonically decreasing function in the LCHA region, Figure 6a suggests that the distribution has been determined from too little data. As shown in Figure 6b, the distribution for 37 10-minute records (the Class 5 loads from the 24-hour simulation) yields a smoother function, but is there enough data to define a representative sample of the loads on the blade? The real test of how much data is required is a comparison of the damage produced by the distributions.

Winterstein and Lange<sup>17</sup> have examined the question of minimum data requirements previously. As

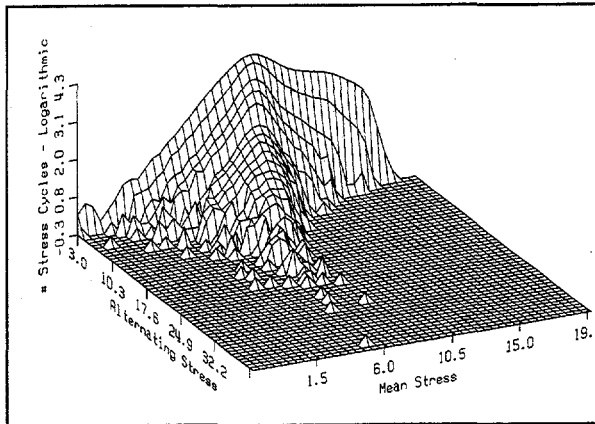


**Figure 6b. Cycle count matrix based on 37 10-minute simulations.**

discussed by them, the answer is highly dependent on a number of variables. Two important variables are the coefficient of variation (COV) that is acceptable in the damage calculation and the fatigue exponent of the blade material. Using the "bootstrap method," they estimated that at least 280 minutes (4.7 hours) are required to define the cyclic load distribution for a composite blade. They assumed that the blade material has a high fatigue exponent (10) and that the target COV for the damage is 0.5. They chose this particular value for the COV because the COV for the strength of the blade material is also about 0.5.

Here, we will use these long simulations to address the question of how much data is sufficient to define the cyclic load distribution.

#### 24-hour Simulation at Row 41

A total of 37 Wind Class 5 simulations are available in the 24-hour ADAMS simulation at Row 41. These simulations were counted as individual files and the damage was determined as described earlier. All 37 simulations were used to determine the average value for this wind speed class. The trajectory of the damage to its average value (nominal damage of 1.0) is shown in Figure 7. In this figure, the average nominal damage versus the number of 10-minute records included in the average is again used to illustrate the trajectory of the accumulated damage to its average. This trajectory is shown in the sequence that was followed during the 24-hour simulation. By sorting the damage first in ascending order, the lower bound trajectory is obtained. Then, by sorting in descending order, the upper bound trajectory is obtained.

As shown in Figure 7, the damage stays within approximately +7 and -25 percent of its average value

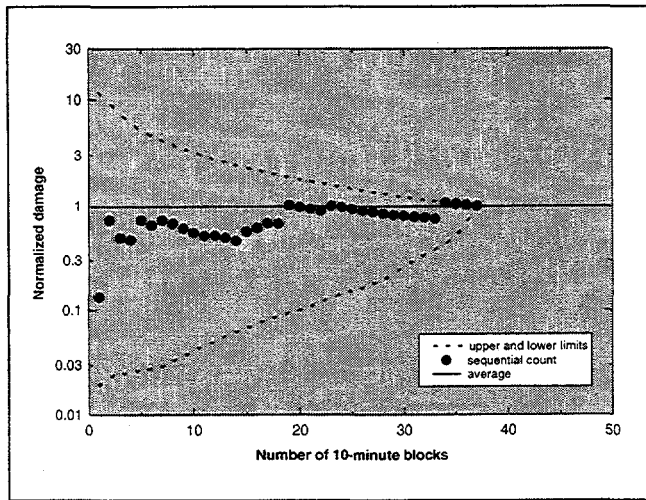


**Figure 7. Wind Class 5 normalized damage trajectory using the 24-hour Row 41 simulation.**

**Table 2. Effect of file counting procedure on damage prediction for Wind Speed Class 5.**

Row	Duration	Description	Normalized Damage		Per Cent Change
			Single	Concatenated	
41	6.2 Hour	24-Hour Simulation	1.00	1.56	56
41	8 Hour	8-Hour Simulation	0.41	0.90	117
37	8 Hour	8-Hour Simulation	1.00	1.05	5
37	2.3 Hour	Measured Data	7.54	8.99	19

after the first 19 10-minute simulations (3.1 hours). This value is in general agreement with the Winterstein and Lange<sup>17</sup> prediction of approximately 280 minutes (4.7 hours). As is shown by the upper and lower bounds, one needs a mix of conditions to predict the average in this time period. At 280 minutes, the lower bound was 80 percent below the average and the upper bound was 30 percent above.

#### **8-hour Simulation at Row 41**

The 48 10-minute YawDyn simulations at Row 41 yielded approximately the same results as the 37 10-minute ADAMS simulations from Wind Class 5 in the 24-hour simulation. At 280 minutes, the upper bound was 67 percent over the average and the lower bound was 90 percent below the average. Of interest is the result that the 8-hour simulation did not converge to the same damage value as the 37 histories within Wind Speed Class 5 of the 24-hour simulation. The 8-hour simulation produced approximately 59 percent less damage. As discussed previously, this result could be anticipated because the long simulations use constant turbulence scaling parameters. Thus, they do not include the time-varying influence of stability and vertical mean shear. The difference between these long runs and those contained within the diurnal simulation is that the stability and shear variability are maintained in the latter.

#### **8-hour Simulation at Row 37**

As shown in Figure 5, the upper bound was 27 percent over and the lower was 66 percent lower at Row 37 at 280 minutes.

#### **LONG TIME SERIES**

As the inflow into a turbine is not steady, long time series cannot be obtained from experimental data. Typically, 10-minute segments of data are all that can be obtained. As discussed in Sutherland and Butterfield,<sup>16</sup> several techniques have been proposed to obtain the long time series that are required to

adequately describe the load spectrum on the turbine at a particular operational state (as described above, at least 4.7 hours of data are required to characterize the loads on composite blades). The first technique is to count each segment as an independent sample, and the second is to concatenate all of the segments into a single file before counting. Standard rainflow counting using the former approach yields many more unclosed cycles than the latter. With the modified rainflow cycle counting algorithm used here, all unclosed cycles are closed. However, they will be shifted to a lower range because they are not matched to the highest high and lowest low in the entire set of data records.

Two classes of "missed cycles" can be examined with the data provided by the long-term simulations presented here. As discussed in Sutherland and Butterfield,<sup>16</sup> most fatigue analyses of wind turbines divide the operation of the turbine into independent operational states. Typically, the operational states include normal operation at a variety of wind speeds (inflow conditions), starting and stopping sequences, and buffeting by high winds. First, we will examine the cycles associated with a normal operation state, i.e., normal operation within Wind Speed Class 5. And, second, we will examine the "transition" or "ground" cycles that are generated by moving between normal operational states.

#### **Normal Operation States**

To examine the effect of single- and concatenated-file counting on damage at a single normal operation state of the turbine (normal operation within the Class 5 wind speed range), all the simulation and experimental data records were counted both ways. The results of these calculations are summarized in Table 2. In this table, the damage has been normalized to the single-file counted damage contained in the 37 10-minute records (6.2 hours) from the 24-hour simulation. As shown in this table, the concatenated file counted scheme always produces greater damage than the single counted scheme. Only in one instance is the change in predicted damage significant; i.e., only for the Row 41 8-hour

simulation is the predicted damage from the concatenated counting scheme over twice as large as that predicted by the single segment counting scheme (typically, fatigue predictions must change by at least a factor of two before their difference is considered to be significant).

#### Transition Cycles

The 24-hour simulation at Row 41 provides the necessary data to examine the transition cycles between normal operation states of the turbine. By concatenating all of the 144 10-minute simulated load histories into a single file, the predicted damage for the diurnal cycle is approximately 8 percent higher than by counting the files separately.

This analysis follows the previous work of Larsen and Thomsen.<sup>18</sup> In an analysis of the transitional load cycles imposed on a turbine blades during a year of operation, they demonstrated that the transition cycles can increase the damage rate by 3 percent in materials with a low fatigue exponents and by 60 percent in materials with a high exponent. This analysis is different from that presented here in that their analysis is base on a different annual wind speed distribution and it includes transient events. Thus, the 60 percent increase cannot be compared directly to the 8 percent increase determined in the 24-hour simulation. However, both simulations indicated that transitional cycles are present and that they should be examined in a fatigue analysis of a turbine blade. Our calculations indicate that for the Micon turbine, the transition load cycle between normal operation states are not significant in the prediction of damage.

#### CONCLUSIONS

The damage calculated from the simulations was considerably less than that determined from 2.3 hours of measured data. An examination of the corresponding load spectra for each case revealed that the simulations lacked the large-amplitude cycles that were present in the observed data and that the slope of distribution in the LCHA region was less. At this time, it is not clear why the simulations are underpredicting the loads on the turbine. Additional research is required to resolve this issue.

For blade materials with high fatigue exponents (i.e., typical U.S. wind turbine blades made of fiberglass), the simulations presented here indicate that at least 4 hours of load history data are necessary to adequately define a representative fatigue spectrum for the normal operation of the turbine. This estimate is highly dependent on the material properties and the target COV for the service lifetime predictions.

Moreover, the load histories contained in this 4-hour sample must reflect a representative sample of the range of expected inflow characteristics as well.

A conservative approach to estimating fatigue damage is to concatenate the available load time histories into a single, continuous record before cycle counting. A comparison between this technique and summing individually-counted load histories indicates that for the Micon turbine, the difference between the two techniques is not significant. However, concatenation is the more conservative approach because it predicts greater damage than the individually-summed approach..

For materials with high fatigue exponents, transition cycles between normal operation states were not found to be important in the damage analyses of the Micon wind turbine blade. As noted by Larsen and Thomsen,<sup>18</sup> the contributions of transition cycles to blade damage is extremely dependent on material properties. Thus, the transition cycles may be an important contributor to the damage incurred on a turbine during operation and they should be included in damage analyses of wind turbines.

#### REFERENCES

1. Kelley, N.D., Wright, A.D., Buhl, M.L., Jr., and Tangler, J.L., "Long-Term Simulation of Turbulence-Induced Loads Using the SNLWIND-3D, FAST2, YAWDYN, and ADAMS Numerical Codes," *16<sup>th</sup> ASME/AIAA Wind Energy Symposium*, in publication, 1997.
2. Kelley, N.D., "Full Vector (3-D) Inflow Simulation in Natural and Wind Farm Environments Using an Expanded Version of the SNLWIND (Veers) Turbulence Code," *Wind Energy 1993*, SED-Vol.14, ASME, 1993.
3. Hansen, A.C., "Yaw Dynamics of Horizontal Axis Wind Turbines," NREL TP-442-4822, National Renewable Energy Laboratory, Golden, CO, 1992.
4. Elliott, A.S., and Wright, A.D., ADAMS/WT: An Industry-Specific Interactive Modeling Interface for Wind Turbine Analysis," *Wind Energy 1994*, SED-Vol.15, ASME, 1994.
5. H.J. Sutherland and L.L. Schluter, "The LIFE2 Computer Code, Numerical Formulation and Input Parameters," *Proceedings of WindPower '89*, SERI/TP-257-3628, 1989.
6. Tangler, J., Smith, B., Kelley, N., and Jager, D., "Measured and Predicted Rotor Performance for the SERI Advanced Wind Turbine Blades," NREL TP-257-4594, National Renewable Energy Laboratory, Golden, CO, 1992.

7. Laino, D.J., and Kelley, N.D., "Investigating the Micon 65 Turbine Using YawDyn With Simulated Turbulence," *Proceedings of WindPower '95*, AWEA, 1995.
8. Buhl, M.L., Jr., Kelley, N.D., Wright, A.D., and Osgood, R.M., "Development of a Full System Dynamics Model of the Micon 65 Wind Turbine Using ADAMS<sup>®</sup>," *Wind Energy 1994*, SED-Vol. 15, ASME, 1994.
9. Højstrup, J., and Nørgård, P., "Tændpibe Windfarm Measurements 1988," RISØ M-2894, Risø National Laboratory, Roskilde, Denmark, 1990.
10. Sutherland, H.J. and Mandell, J.F., "Application of the U.S. High Cycle Fatigue Data Base to Wind Turbine Blade Lifetime Predictions," *Energy Week 1996, Book VIII: Wind Energy*, ASME, 1996.
11. Mandell, J.F., Reed, R.M., Samborsky, D.D., and Pan, Q., "Fatigue Performance of Wind Turbine Blade Composite Materials," *Wind Energy 1993*, SED-Vol.14, ASME, 1993.
12. Downing, S.D. and Socie, D.F., "Simple Rainflow Counting Algorithms," *Int'l J. of Fatigue*, Vol.4, N.1, 1982.
13. Schulter, L.L. and Sutherland, H.J., "Rainflow Counting Algorithm for the LIFE2 Fatigue Analysis Code," *9<sup>th</sup> ASME Wind Energy Symposium*, SED-Vol.9, ASME, 1990.
14. Sutherland, H.J. and Kelley, N.D., "Fatigue Damage Estimate Comparisons for Northern European and U.S. Wind Farm Loading Environments," *Proceedings of WindPower '95*, AWEA, 1995.
15. Tangler, J., Smith, B., Jager, D., McKenna, E., and Allread, J., "Atmospheric Performance Testing of the Special-Purpose SERI Thin Airfoil Family: Preliminary Results," *Proceedings of WindPower '89*, AWEA, 1989.
16. Sutherland, H.J. and Butterfield, C.P., "A Summary of the Workshop on Fatigue Prediction Life Methodologies for Wind Turbines," *Proceedings of WindPower '94*, AWEA, 1994.
17. Winterstein, S.R., and Lange, C.H., "Load Models for Fatigue Reliability from Limited Data," *Wind Energy-1995*, SED-Vol. 16, ASME, 1995.
18. Larsen, G. and Thomsen, K., "A Simple Approximative Procedure for Talking into Account Low Cycle Fatigue Loads," *Proc. IEA 4<sup>th</sup> Symposium of Wind Turbine Fatigue*, IEA, 1996.